# EXPERIMENTAL STUDIES OF ACOUSTIC SCATTERING BY CYLINDRICAL OBJECTS

V F Humphrey (1) & C Beckett (2)

(1) School of Physics, University of Bath, Claverton Down, Bath BA2 7AY, UK
(2) BAeSEMA Ltd, Unit D1, Marabout Industrial Estate, Dorchester, UK

## 1. INTRODUCTION

The acoustic scattering from discrete objects immersed in a fluid has received considerable attention for a number of years. For regular bodies a number of approaches including normal mode solutions and the T matrix have been used to predict the scattered field [1]. Recent attention has concentrated on the interpretation of the predictions of these theories in terms of the different types of wave propagating in and around the scattering body and the effects of resonances produced by these waves on the scattering behaviour [2]. The scattering properties of less regular bodies can now be investigated theoretically by a combination of finite element and boundary element techniques.

A range of carefully controlled experimental measurements are required to complement and provide verification of these theoretical developments. The required precision is most easily obtained under laboratory conditions and many tests have been carried out above 200kHz. However these measurements are often made on samples which are large compared with a wavelength or on small targets for which it is difficult to include structure. This paper describes experimental results obtained at lower frequencies (10-200kHz) on structures comparable with a wavelength in size using a parametric array as an acoustic source.

## 2. EXPERIMENTAL TECHNIQUE

The experimental system used is shown in Figure 1 and has been described in detail elsewhere [3,4]. The waveform applied to the 50mm diameter transducer consists of a 920kHz carrier pulse with a raised cosine-bell envelope (Figure 2(b)). The nonlinear propagation of this pulse through the water generates, by self-demodulation [5], a low-frequency secondary pulse (Figure 2(c)) that is used experimentally. The resulting wavefield is detected by a hydrophone, filtered and recorded. The application of FFT techniques enables measurements to be made over a wide frequency range using the broad-band demodulated pulses. The length and frequency content of the demodulated pulse can be adjusted by altering the frequency of the raised cosine bell envelope. This enables the scattering response to be analysed over a wide frequency range by using two or three different modulation envelopes.

The acoustic measurements were made in a laboratory test tank 1.2 x 1.2 x 1.8m in size. The parametric array was truncated at a range of about 0.6m by an acoustic low pass filter that attenuated the carrier frequency by at least 30dB. This prevented further generation of the low frequency pulse and ensured that the receiving hydrophone was operated in region free of high amplitude primary waves so that errors due to hydrophone nonlinearity were avoided. The experimental signals were measured with a Brüel and Kjær 8103 hydrophone and then passed through a low pass filter to remove any remaining carrier signal. The resultant signals were amplified, captured with an ANALOGIC DATA 600E and passed to a PC for further processing and storage.

For normal incidence measurements the cylindrical samples were suspended vertically on the acoustic axis of the transducer and the hydrophone was positioned at an angle $\phi$ and range $r$ to record the scattered signal (Figure 3(a)). For oblique incidence measurements the cylinders/ cylindrical shells were suspended horizontally at an angle $\alpha$ to the axis and the hydrophone was positioned in the direction of the geometrical reflection (Figure 3(b)). The narrow beams produced by the parametric source meant that the samples used were effectively infinite in length.

The measurement technique used the stability of the acoustic output to enable any coherent background signal in the tank to be subtracted leaving only the scattered signal due to the test object. To enhance this technique the signal to noise ratio was improved by averaging each signal over a number of pulses prior to further processing or analysis. The number of pulses averaged varied with the object, but typically 256 pulses were used. First the total field was measured at a known observation range and angle (Figure 4(a)). Then the test object was removed and the coherent background recorded (b). This was subtracted from the total signal to leave only the scattered signal (c). The hydrophone was then moved to the position of the centre of the scattering object and the incident signal was recorded (d). Fourier analysis of the resulting waveforms enabled the scattering characteristics of the cylinder to be obtained as a function of frequency. The experimental results are presented in terms of the form function which was obtained from the ratio of the spectrum of the scattered signal to that of the incident signal, multiplied by $\sqrt{2r/a}$ where a was the external radius of the cylinder / cylindrical shell.

## 3. THEORETICAL PREDICTIONS

The experimental results are compared with the predictions of Normal Mode Series solutions for cylinders and shells [6-8]. These solutions assume that the incident wavefield is a plane wave. For measurements made under laboratory conditions this is generally not the case and can affect the measured form function significantly. The effects of the non-plane wave nature of the wavefield may be considered on two levels. For normal incidence the scattered field of a cylinder would be expected to fall off as $1/\sqrt{r}$ with distance from the cylinder. Simple geometrical arguments indicate that for an incident spherical wave and a perfect cylindrical reflector there will be an extra fall off $\sqrt{z/(z+r)}$, where z is the distance from the source to the cylinder, due to cylindrical spreading in the plane of the cylinder axis. This geometrical spreading factor can be used to obtain a modified theoretical form function $f_{geo}$ [4,9].

A more rigorous approach is to consider the incident wavefield as consisting of an angular spectrum of plane waves. Each plane wave is incident on the cylinder from a different direction and therefore results in a slightly different scattered wave at the observation position. The total scattered wavefield is simply the integral over these scattered components. A full development must take into account the plane wave spectrum of the parametric source. This integral approach leads to a modified prediction for the observed form function [4,9].

## 4. EXPERIMENTAL SCATTERING RESULTS

### 4.1 Solid Cylinder

Figures 5(a) and 5(b) show the form function measured at 180° (back scatter) and at 90° for an aluminium cylinder 13mm in radius as a function of ka. The detailed broad-band nature of the results which cover the frequency range 10kHz to 270kHz should be noted. The theoretical predictions for a single plane wave (dotted line) can be seen to be significantly higher than the observed values over the entire frequency range. The agreement with the modified theory which allows for the plane wave spectrum of the source (solid line) is very good over most of the frequency range. It is important to note that the modified theory not only predicts the amplitude levels but also shows some sharp resonances seen in the experimental data but not on the plane wave result. These are attributed to helical waves excited by plane wave components incident on the cylinder at non-normal incidence. The average reduction in the amplitude of the modified form function by a factor of about 0.85 can be attributed to additional cylindrical spreading of the scattered wavefield in the xz plane. The observed reduction agrees with that which would be expected if the effective acoustic centre of the array were half way between the transducer and acoustic filter. The reduced level of agreement at higher frequencies is possibly due to the inadequacy of the line array model used for the parametric source in these calculations [4].

This experimental technique can also be applied to bistatic measurements for scattering at oblique incidence. An example of this type of application can be seen in the results shown in Figure 6 for the case of a solid aluminium cylinder insonified at an angle of 30°. In this configuration the accuracy with which the cylinder can be orientated is much more significant. It is believed that the cylinder can be positioned to within 1° but for this angle of incidence the form function varies rapidly with angle of incidence. The results do however show reasonable agreement. For this arrangement it is more difficult to compensate for the plane wave spectrum of the incident field.

### 4.2 Circular Cylindrical Shells

Figure 7 illustrates a selection of experimental results obtained for scattering by a stainless steel shell with an inner radius (b) of 12.4mm and outer radius (a) 12.7mm giving a b/a ratio of 0.976. In these results the plane wave prediction is shown as a dotted line and a corrected form function calculated using geometrical spreading as a solid line. Figures 7 (a) and (b) compare the normal incidence back scattered form function for a water filled and an air filled shell. The air-filled shell form function clearly shows regular dips due to resonances of the first symmetric ($S_0$) Lamb wave in the shell. The water filled shell, by comparison, produces a much more complex result as a consequence of resonances of the water column. The good agreement between experiment and the geometrically corrected form function should be noted. Figure 7(c) presents a similar result for the air filled shell but for an observation angle of 90°.

## 5. CONCLUSIONS

The results presented show that the experimental facility can be used to make broad-band measurements of acoustic scattering for low ka values in the laboratory. The results are in good agreement with theoretical predictions if allowance is made for the plane wave spectrum of the source. The technique has considerable potential and can be extended to observations of less-regular scattering bodies [10], or in principle to model scattering from irregular bodies such as sediment particles. It can also be used to study systems containing a number of scatterers.

## 6. ACKNOWLEDGEMENTS

This work has been carried out with the support of the Procurement Executive of the Ministry of Defence and the Defence Research Agency, UK.

## 7. REFERENCES

[1] R H Hackman, "Acoustic scattering from elastic solids" in *Physical Acoustics XXII*, edited by A D Pierce & R N Thurston, Academic Press, (1993).

[2] L Flax, G C Gaunaurd & H Überall, "Theory of resonance scattering" in *Physical Acoustics XV*, edited by W P Mason, R N Thurston, NewYork, Academic Press, (1981).

[3] V F Humphrey, "The measurement of acoustic properties of limited size panels by use of a parametric source", *J. Sound Vib.*, **98**, p67 - 81, (1985).

[4] C Beckett, "Studies of acoustic scattering using a parametric array", PhD Thesis, University of Bath, (1992).

[5] H O Berktay, "Possible exploitation of non-linear acoustics in underwater transmitting applications", *J. Sound Vib.*, **2**, p435 - 461, (1965).

[6] J J Faran, "Sound scattering by solid cylinders and spheres", *J. Acoust. Soc. Am.*, **23**, p405 - 418, (1951).

[7] L Flax, V K Varadan & V V Varadan, "Scattering of an obliquely incident wave by an infinite cylinder", *J. Acoust. Soc. Am.*, **68**, p1832 - 1835, (1980).

[8] R D Doolittle & H Überall, "Sound scattering by elastic cylindrical shells", *J. Acoust. Soc. Am.*, **39**, p272 - 275, (1966).

[9] V F Humphrey & C Beckett, "The application of a parametric array to scattering studies in the laboratory", in *Frontiers of nonlinear acoustics: Proceedings of 12th ISNA*, p265 - 270, London, Elsevier (1990).

[10] P A Chinnery and V F Humphrey, "Resonances in acoustic scattering by cylindrical objects", in this volume.

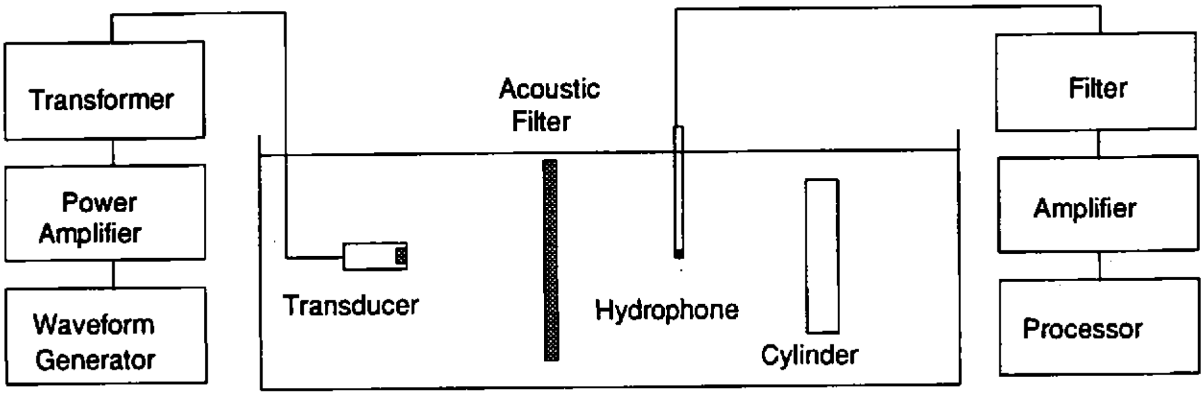


Figure 1. Experimental arrangement.

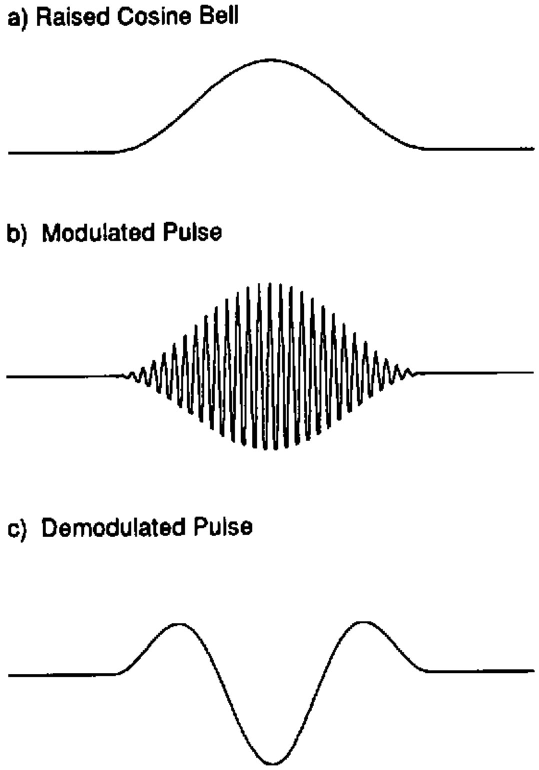


Figure 2. Waveforms used in the experimental system.

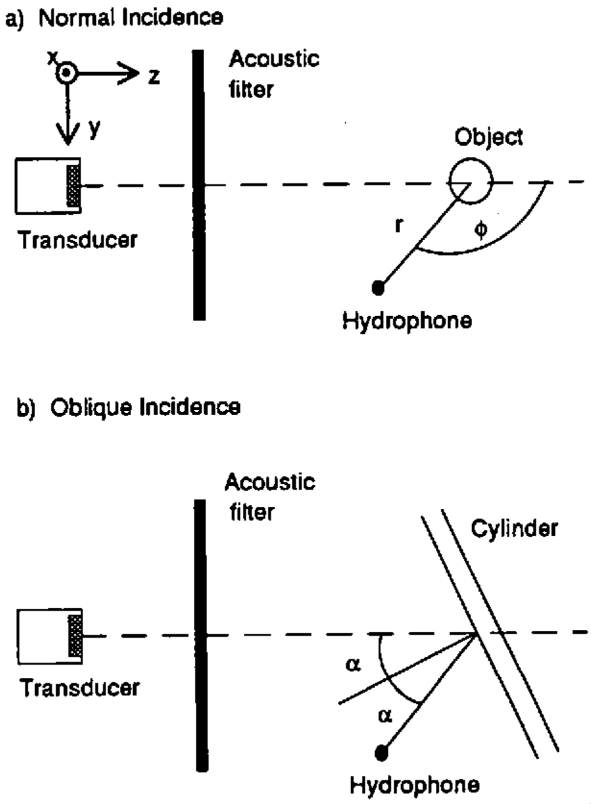


Figure 3. Experimental arrangements (viewed from above) for scattering measurements at normal incidence (a) and oblique incidence (b), showing the angles $\phi$ and $\alpha$.

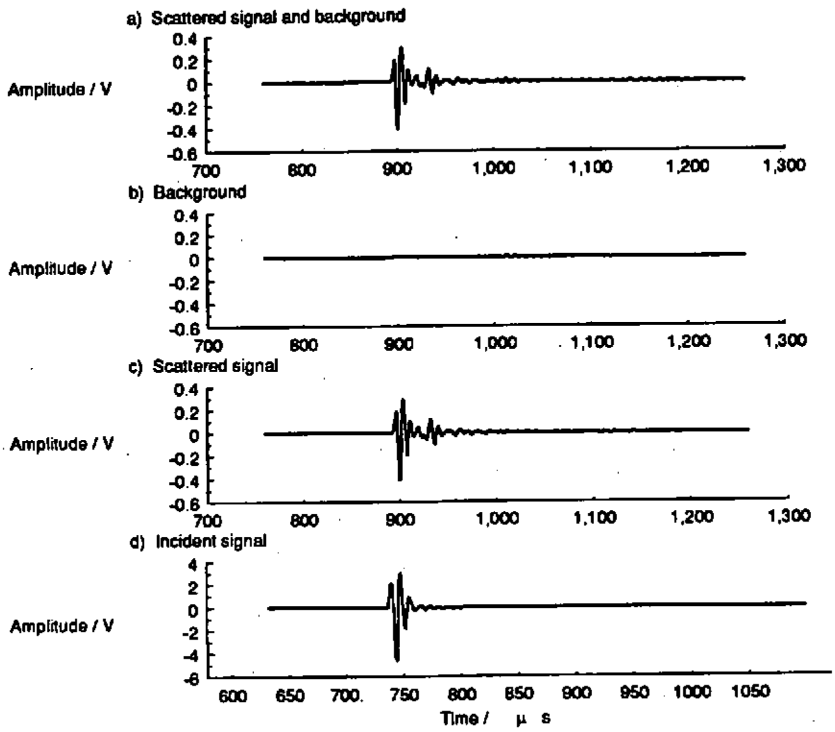


Figure 4. Experimental waveforms obtained for scattering by a solid aluminium cylinder, observed at 90°, for an incident pulse based on a 100kHz envelope.

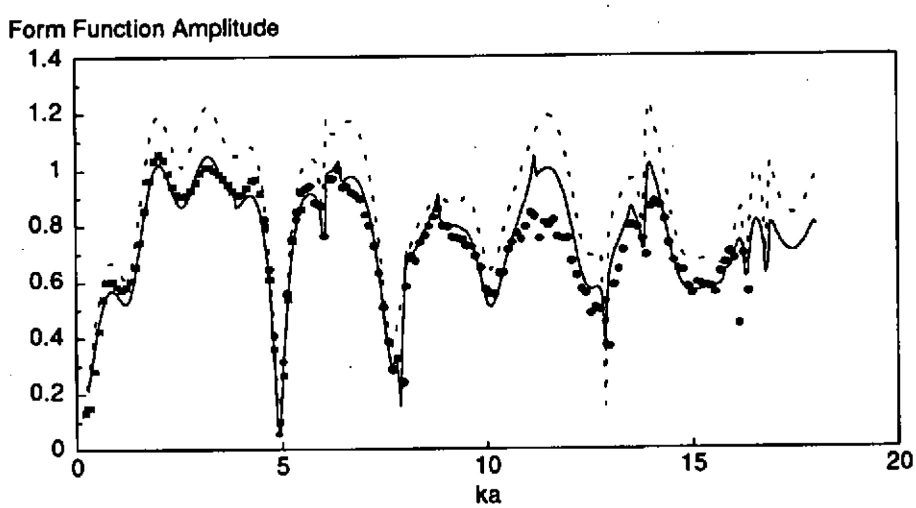


Figure 5(a). Form function amplitude for a solid aluminium cylinder, wavefield incident at normal incidence, observed at 180°; plane wave theory (dotted line), plane wave spectrum theory (solid line) and experiment (points).

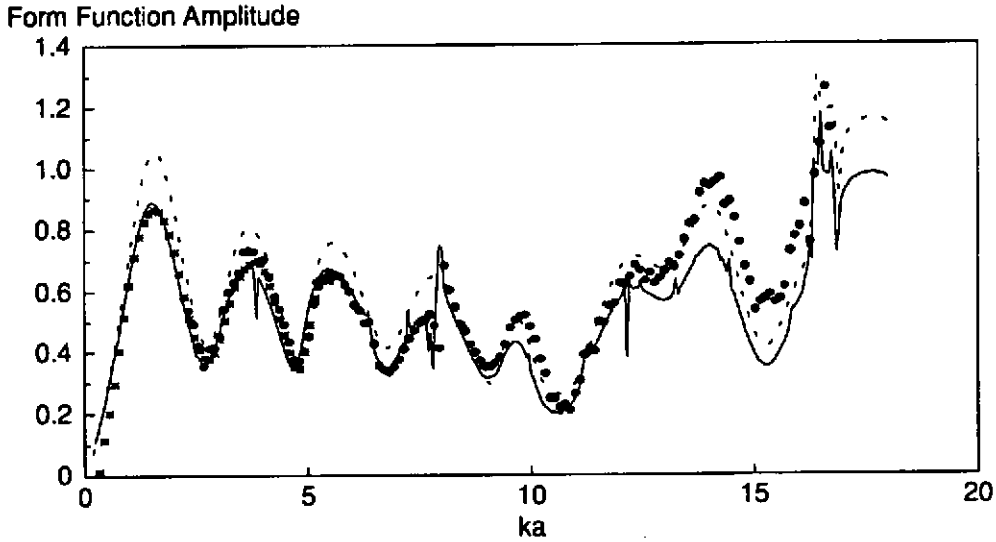


Figure 5(b). Form function amplitude for a solid aluminium cylinder with a=13mm, wavefield incident at normal incidence, observed at 90°; plane wave theory (dotted line), plane wave spectrum theory (solid line) and experiment (points).

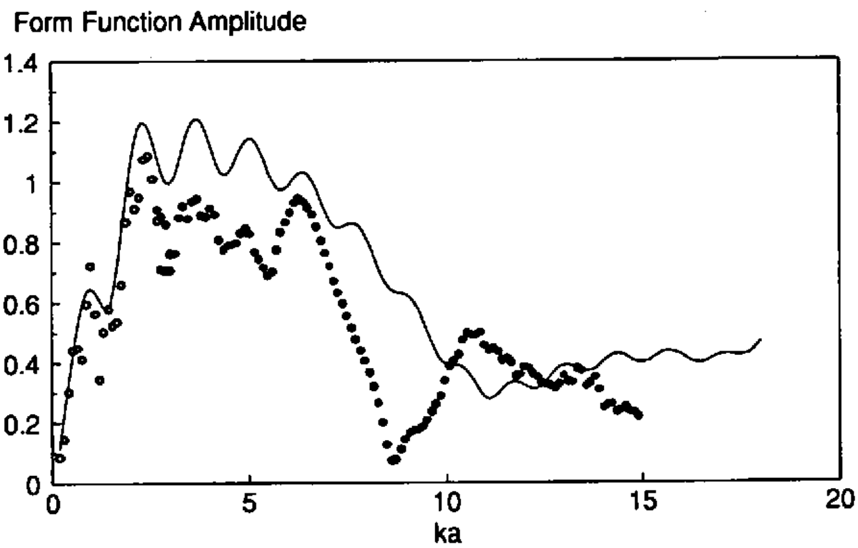


Figure 6. Form function amplitude for a solid aluminium cylinder for an angle of incidence ($\alpha$) of 30°, measured at a range of 0.3m; plane wave theory (solid line) and experiment (points).

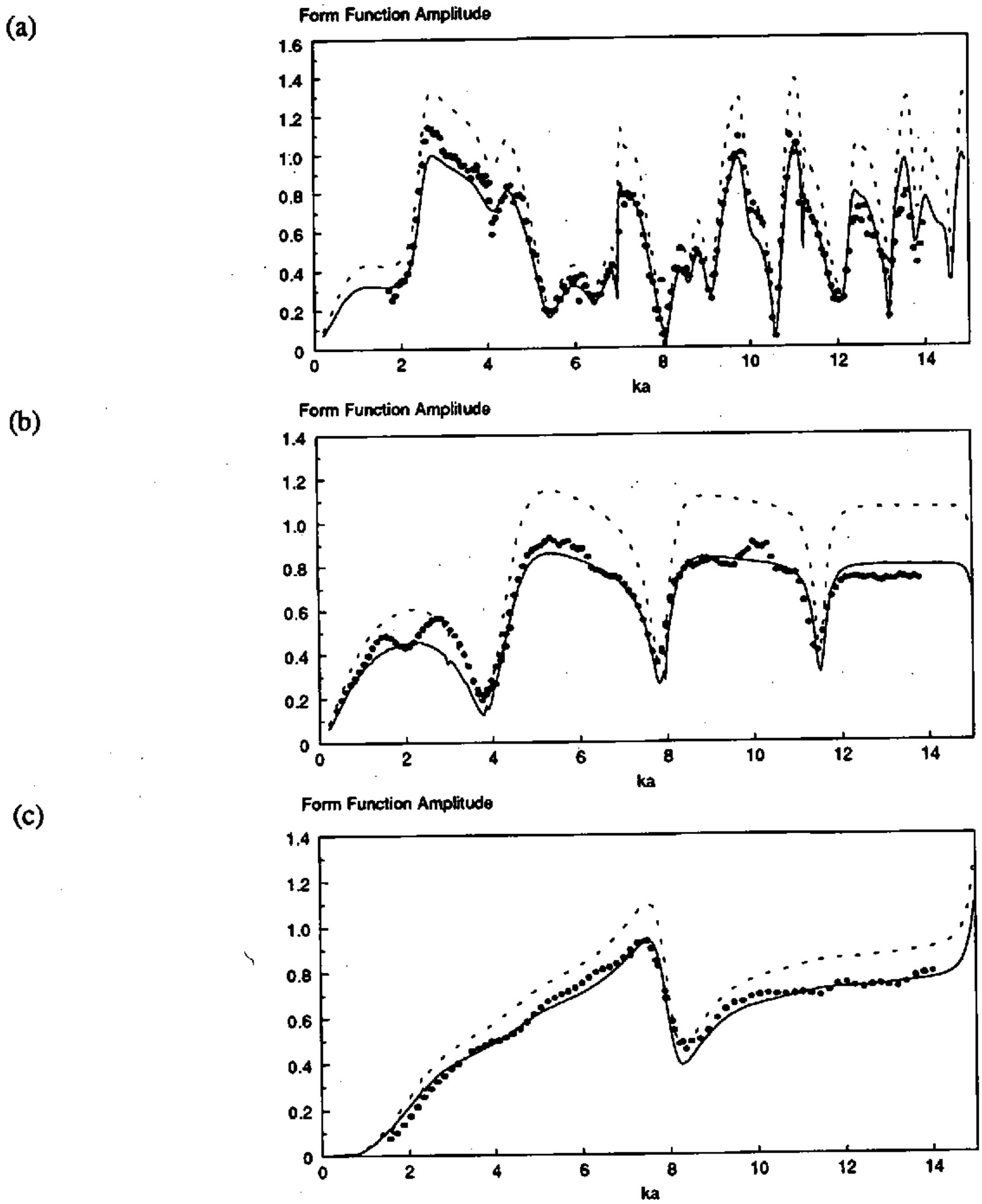


Figure 7. Form function amplitude for a cylindrical stainless steel shell with a b/a ratio 0.976 for normal incidence; plane wave theory (dotted line), geometrically corrected theory (solid line) and experiment (points). (a) water filled shell observed at $\phi=180°$; (b) air filled shell observed at $\phi=180°$ and (c) air filled shell observed at $\phi=90°$.